JJEE

Volume 12 | Number 2 | June 2026 | Pages 314-323

Jordan Journal of Electrical Engineering

ISSN (print): 2409-9600, ISSN (online): 2409-9619

Homepage: jjee.ttu.edu.jo

Energy Consumption Forecasting with PSO-Optimized LSTM Networks

Lahoucine Oumiguil[1*], Ali Nejmi[2], Mohamed Baite[2], Youssef Sadik[2]

[1, 2, 3, 4] Automatic and Energy Conversion Team (EACE), Faculty of Sciences and Technics, Sultan Moulay Slimane University, Beni Mellal, Morocco

E-mail: oumiguil.1992@gmail.com

Received: Oct 18, 2025 *Revised: Jan 06, 2026* *Accepted: Jan 19, 2026* *Available online: Jun 15, 2026*

***Abstract*—** Accurate energy consumption forecasting is crucial for managing and optimizing modern power systems, especially as renewable energy sources become more prevalent and grids grow more complex. This paper introduces a new hybrid model that combines Particle Swarm Optimization (PSO) with Long Short-Term Memory (LSTM) neural networks, significantly improving forecasting accuracy. The main innovation is using PSO to dynamically tune LSTM hyperparameters such as layers, neurons, learning rate, and dropout rate, addressing the limitations of trial-and-error methods. The PSO-LSTM model is thoroughly tested with real data from the Roche Plate microgrid, showing superior results with an MAE of 59.885 Wh and an RMSE of 83.783 Wh, representing a 41.6% improvement over standalone LSTM models. By effectively modeling complex, nonlinear energy consumption patterns, this approach supports better decision-making and resource management for microgrids, especially in isolated areas with intermittent renewable energy. The findings highlight the model's potential to enhance smart grid management and facilitate the shift to sustainable energy systems.

***Keywords*—** Particle swarm optimization; LSTM; Energy consumption forecasting; Microgrid; Deep learning.

1. INTRODUCTION

Global electricity consumption is rising rapidly, and the International Energy Agency (IEA) has indicated that demand growth is expected to reach around 4% in 2024 (up from 2.5% in 2023) and remain near 4% in 2025, increasing pressure on power systems to expand capacity while maintaining reliability [1]. This acceleration is especially consequential for islands, which often operate under tight technical and economic constraints, including limited interconnection to mainland grids, vulnerability to extreme weather events, and stronger exposure to fuel-price volatility due to import dependence [2].

France has responded to these challenges by planning the transition of its overseas territories since 2015, with the objective of energy self-sufficiency by 2030 for its overseas departments; however, despite strong renewable resources, territories such as La Réunion have historically remained highly dependent on fossil-based generation [3]. Microgrids are therefore increasingly viewed as a practical pathway to electrify and stabilize isolated communities such as Mafate, provided that operational control and planning tools are sufficient to prevent imbalance-driven outages. In renewable-rich microgrids, forecasting becomes a foundational function because it directly affects dispatch decisions, storage

* Corresponding author

DOI: https://doi.org/10.5455/jjee.204-1760787217

scheduling, reserve allocation, and reliability management under uncertainty[4]. Recent research has made substantial progress in short-term solar irradiance and photovoltaic (PV) power forecasting, which is critical where PV constitutes a dominant or rapidly growing share of local generation. A recurring finding is that irradiance variables strongly influence PV output estimates, so improved irradiance prediction can lead to more accurate PV production forecasts and more efficient energy management [5]. For instance, Wojtkiewicz et al. [6] present hour-ahead solar irradiance forecasting using multivariate Gated Recurrent Units (GRUs), underlining the suitability of gated recurrent models for short-horizon solar prediction.

A strong trend in the literature is the emergence of hybrid deep learning architectures that combine complementary model classes to capture both temporal dependence and complex nonlinear feature interactions in weather-to-power relationships[7]. Multiple GRU-centered approaches have been reported for short-term PV forecasting, including a GRU-CNN model [8] and GRU-based PV forecasting under environmental variability [9], both of which target the volatility inherent in solar generation. LSTM methods remain prominent as well, with Cheng et al. [10] demonstrating that LSTM-based models can capture intra-hour variation and support one-day-ahead solar power forecasting. More recently, Ibrahim et al. [11] proposes a CNN-LSTM autoencoder approach for short-term PV power generation forecasting, emphasizing the operational value of forecasting for stabilizing power systems and improving energy storage management.

Beyond pure neural hybrids, recent studies increasingly integrate deep networks with structured-data learners to improve accuracy and robustness across operating regimes. The literature highlights the potential of augmenting deep learning pipelines with XGBoost [12], motivated by its effectiveness in handling tabular features and refining predictive outputs when combined with neural representations. Dimitropoulos et al. [13] illustrate this broader hybridization direction in energy-community settings by comparing machine learning and deep learning approaches for short-term PV production forecasting. At the architectural level, Al-Ali et al. [14] propose a CNN-LSTM-Transformer hybrid, aiming to leverage CNN-based feature extraction, sequence learning, and attention mechanisms within a unified framework for solar energy output forecasting.

Alongside these PV-focused developments, forecasting microgrid demand remains equally critical because demand uncertainty compounds renewable uncertainty and directly affects real-time balancing decisions. In previous work by the authors, a hybrid ARIMA-GRU approach was developed for microgrid energy-consumption forecasting by integrating ARIMA residual learning with GRU's nonlinear modeling capability [15]. This result supports the broader conclusion that hybrid time-series models can outperform single-paradigm approaches by capturing both linear structure and nonlinear dynamics in microgrid data.

Motivated by the operational needs of island microgrids and the demonstrated benefits of hybrid learning strategies, this study focuses on microgrid energy-consumption forecasting using a hybrid PSO-LSTM framework. The aim is to exploit LSTM's strength in modeling long-term dependencies in demand time series while using Particle Swarm Optimization (PSO) to systematically tune hyperparameters and improve robustness, thereby supporting more reliable operation and planning in isolated, renewable-rich microgrids.

2. METHODOLOGY

The proposed method integrates Particle Swarm Optimization (PSO) with Long Short-Term Memory (LSTM) networks to perform short-term energy forecasting of microgrid consumption over a 24-48 hour horizon. PSO optimizes key hyperparameters of the LSTM, including the number of layers, neurons per layer, learning rate, and dropout rate. The goal of the optimization is to reduce forecasting errors, which can be measured by metrics like Mean Absolute Error (MAE) or Root Mean Squared Error (RMSE). After optimization, the LSTM model is trained on historical energy consumption and weather data, and its effectiveness is assessed using a separate test set.

1.1. PV System

The experimental stand-alone microgrid deployed at Roche Plate couples photovoltaic (PV) generation with battery-based energy storage to supply electricity to three residential dwellings in an isolated, non-interconnected context (see Fig. 1) [16]. The PV plant has a total installed peak capacity of 7 kWp, implemented as two PV strings of 3.5 kWp each, interfaced through MPPT charge controllers and an inverter/charger that delivers AC power to end users. System operation is instrumented by recording PV power at the two solar regulators (P_{pv1}, P_{pv2}) and the inverter output supplying the local network (P_{out}), while residential electricity use is characterized through sub-metered domestic circuits/appliance groups (e.g., refrigeration/freezing, washing, lighting, entertainment devices, and general sockets).

Fig. 1. Aerial view of the microgrid showing the battery pack and the acquisition devices at the center, with the loads positioned at each of the three ends [16].

1.2. Data Collection and Preprocessing

The study utilized hourly energy consumption and weather data (temperature, solar irradiation, wind speed, relative humidity, and pressure) collected from May to December 2020. As shown in Table 1, temperature demonstrated the strongest positive correlation with energy consumption (0.41), followed by wind speed (0.30) and solar irradiation (0.27), while relative humidity (-0.02) and pressure (-0.19) showed negligible or weak negative correlations. Based on these results, temperature, solar irradiation, and wind speed were selected as the most relevant input features. The dataset underwent Min-Max normalization to scale values between 0 and 1, and missing values were addressed through linear interpolation for gaps shorter than 3 hours. The preprocessed data was structured into 24-hour sequences, with the three key weather parameters as inputs and the subsequent hour's energy consumption as the target output. To ensure a comprehensive evaluation, the dataset was split into training (80%) and testing (20%) sets, keeping the chronological order intact. Furthermore, 20% of the training data was reserved for validation. The final dataset included 4661 training samples and 1166 test samples, representing a variety of seasonal patterns over the 8-month collection period. This preprocessing method preserved the temporal relationships while preparing the data for effective model training and assessment.

Table 1. The Pearson correlation coefficient between energy consumption and weather variables.

	Temperature	Wind speed	Solar irradiation	Relative humidity	Pressure
Pearson correlation coefficient	0.41	0.3	0.27	-0.02	-0.19

1.3. Long Short-Term Memory Architecture

The LSTM model is a type of recurrent neural network (RNN) designed to better retain information over long sequences. It features special memory units that can update the hidden state, providing feedback at each neuron. An RNN's output depends on both current inputs and previous inputs, allowing LSTM to capture temporal relationships in long-term data. Its internal memory units and gate mechanisms help prevent issues like exploding and vanishing gradients during training. The LSTM structure includes four main components: the input gate, output gate, forget gate, and cell state. These gates regulate how information is stored and updated within the cell state. Figure 2 illustrates the architecture of an LSTM cell, and the computation process is explained as follows [17]:

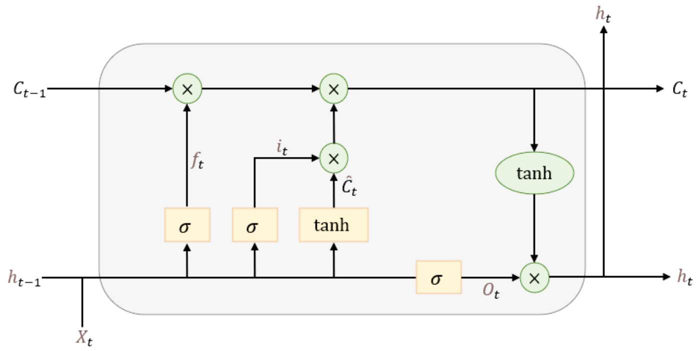

Fig. 2. Structure of long short-term memory cell.

$$i_t = \sigma(W_i x_t + U_i h_{t-1} + b_i) \quad (1)$$
$$f_t = \sigma(W_f x_t + U_f h_{t-1} + b_f) \quad (2)$$
$$o_t = \sigma(W_o x_t + U_o h_{t-1} + b_o) \quad (3)$$
$$\hat{C}_t = tanh(W_c x_t + U_c h_{t-1} + b_c) \quad (4)$$
$$C_t = f_t \otimes C_{t-1} + i_t \otimes \hat{C}_t \quad (5)$$
$$h_t = o_t \otimes tanh\,(C_t) \quad (6)$$

In the equations above, i_t, f_t and o_t These are the three gates: input, output, and forget gates located at each time step. t, The W_i , W_f and W_o: denote the weight matrices from the input, forget and output gates to the input, respectively. The b_i, b_f and b_o these are the biases of the input, forget, and output gates, respectively. The U_i, U_f adenote the weight matrices for the input, forget, and output gates to the hidden state respectively. σ is a logistic sigmoid function and $\otimes$ denotes the element-wise multiplication of two vectors. x_t is a vector that is in the input layer of the LSTM. h_t is an output vector from the hidden layer located within the LSTM unit at time t. C_t denotes the current cell state and $\hat{C}_t$ denotes the new candidate value for the next cell state. h_{t-1} denotes the previous state and is defined by the forget gate, f_t, by how much is passed to the next state. C_{t-1} indicates the process of updating the previous cell state to the new one state, C_t.

The basic LSTM structure was created to model temporal dependencies in energy consumption data effectively. It starts with an input layer designed for 24-hour sequences of three weather parameters: temperature, solar irradiation, and wind speed. Two stacked LSTM layers, each with 50 neurons, form the core to capture both short-term and long-term patterns. A dropout layer with a rate of 0.5 is placed between these layers to reduce overfitting by randomly deactivating neurons during training. The final layer is a dense output with linear activation to predict energy consumption for the next hour. The model uses the Adam optimizer with its default learning rate of 0.001 and Mean Squared Error as the loss function. This setup offers a solid baseline, balancing model complexity and computational efficiency while learning meaningful temporal relationships. Batch normalization is applied between layers to stabilize and speed up training. The recurrent connections and gating in the architecture help it selectively remember or forget information over time, making it well-suited for energy forecasting.

1.4. PSO-based Hyperparameter Optimization

PSO is an optimization method inspired by how birds flock or fish school. It begins with a group of candidate solutions, known as particles, that navigate the search area to find the best overall solution. Each particle has a position and velocity, which are adjusted each cycle based on the particle's personal best and the best position discovered by the entire swarm[18]. The main steps of the Particle Swarm Optimization algorithm are as follows:

1. Start with a population of particles randomly placed in positions and velocities.
2. Assess each particle's fitness using a specified objective function.
3. Update the personal best position of the particle and the global best position.
4. Update each particle's velocity and position according to the following methods equations:

$$v_i^{k+1} = \omega v_i^k + c_1 r_1 \left(p_i^k - x_i^k\right) + c_2 r_2 \left(p_g^k - x_i^k\right) \quad (7)$$

$$x_i^{k+1} = x_i^k + v_i^{k+1} \quad (8)$$

where $v_i^{k+1}$is the velocity of particle i at iteration k, x_i^k is the position of particle i at iteration k, r_1 and r_2 are random numbers between 0 and 1, c_1 and c_2 are cognitive and social acceleration coefficients, and ω is the inertia weight. Continue repeating steps 2-4 until a stopping condition is reached, such as hitting a maximum number of iterations or achieving a desired fitness level.

The LSTM architecture's performance was enhanced through PSO to determine optimal hyperparameters systematically. The optimization process focused on four critical parameters: the number of LSTM layers (search space: 1-3), neurons per layer (20-100), learning rate

(0.0001-0.01), and dropout rate (0.1-0.5). A swarm of 30 particles was initialized with random positions and velocities within these defined bounds. Each particle's fitness was evaluated using the Root Mean Square Error (RMSE) on a validation set comprising 20% of the training data. The PSO algorithm employed cognitive and social coefficients (c_1 = c_2 = 1.49) along with an inertia weight (ω = 0.72) to balance exploration and exploitation during the search process. At each iteration, particles updated their velocities by considering their personal best positions and the swarm's global best, following the standard PSO velocity update equation. This dynamic adjustment allowed the swarm to efficiently navigate the hyperparameter space while avoiding premature convergence to local optima. The optimization ran for 100 iterations or until meeting an early stopping criterion, ultimately identifying the hyperparameter combination that minimized forecasting error. This automated approach eliminated the need for manual tuning while ensuring the LSTM model achieved optimal performance for the specific forecasting task. The final optimized architecture demonstrated improved generalization capability compared to the baseline configuration, particularly in handling the microgrid's nonlinear consumption patterns and weather-dependent variability.

1.5. Model Evaluation

Forecasting performance is assessed using standard accuracy metrics like Mean Absolute Error (MAE) and Root Mean Square Error (RMSE)[19]. These metrics quantitatively measure the difference between predicted and actual values, as explained below:

$$MAE = \frac{1}{N}\sum_{i=1}^{N}\left|(y_{predicted} - y_{actual})\right| \tag{9}$$

$$RMSE = \sqrt{\frac{1}{N}\sum_{i=1}^{N}(y_{predicted} - y_{actual})^2} \tag{10}$$

Here, **N** refers to the sample size or the amount of training data sets, $\mathbf{y_{predicted}}$ and $\mathbf{y_{actual}}$ are the predicted and actual values, respectively. The MAE is a widely used statistical metric that calculates the average absolute difference between predicted and actual values, indicating the model's accuracy. RMSE assesses the standard deviation of these differences, highlighting larger errors because of its mathematical characteristics. Typically, lower MAE and RMSE values indicate a more precise predictive model.

3. RESULTS AND DISCUSSION

3.1. Performance Evaluation of LSTM Model

The comparative analysis of forecasting models, LSTM, SVR, and ANN, revealed significant differences in forecasting accuracy. As summarized in Table 2, the LSTM model achieved the lowest MAE (101.684 Wh) and RMSE (143.547 Wh), outperforming both SVR (MAE: 137.986 Wh, RMSE: 187.252 Wh) and ANN (MAE: 131.912 Wh, RMSE: 175.364 Wh). This outstanding performance stems from LSTM's innate capacity to identify temporal dependencies and nonlinear patterns in energy consumption time series. Unlike conventional machine learning models, LSTM's recurrent structure and memory gates facilitate the effective learning of long-term trends and short-term fluctuations, which are essential in microgrid settings with fluctuating renewable sources and load profiles.

Table 2. Summary of model performance evaluation.

Algorithm	MAE [Wh]	RMSE [Wh]
SVR	137.986	187.252
ANN	131.912	175.364
LSTM	101.684	143.547

Figure 3a illustrates the hourly forecastings of the three models against actual consumption over a representative day. The LSTM forecastings align closely with real data, particularly during peak demand periods (e.g., 18:00-22:00), where SVR and ANN exhibit significant deviations. The Absolute Percentage Error (APE) plot (Fig. 3b) reinforces this observation: LSTM maintains errors below 10% for most hours, while ANN and SVR reach up to 15% and 20%, respectively. Such precision is critical for microgrid operators to avoid under- or over-generation, ensuring stable grid operation and efficient energy storage utilization.

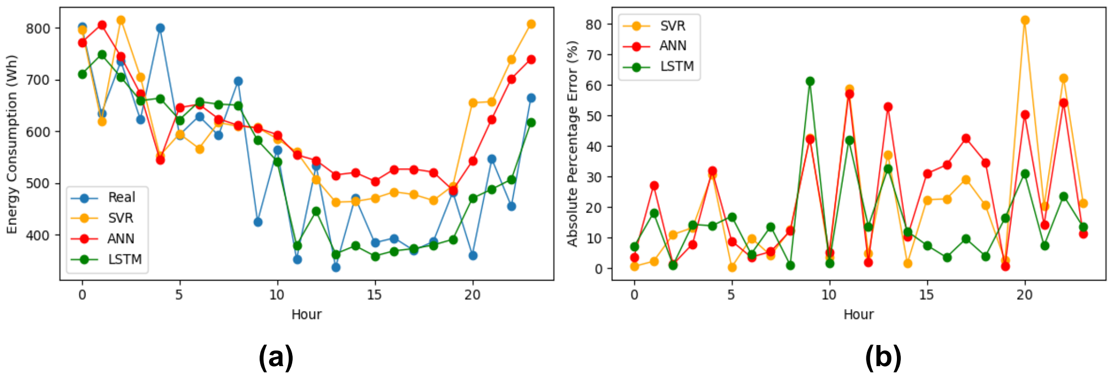

Fig.3. The performance of the LSTM, ANN, and SVR models: a) Real energy consumption and energy forecasting a full day; b) Absolute Percentage Error in energy forecasting throughout the day.

3.2. Performance Evaluation of PSO-LSTM Model

To further improve forecasting accuracy, the LSTM model was combined with PSO for hyperparameter tuning. The resulting PSO-LSTM model showed significant improvements over both the baseline LSTM and other variants from the literature (see Table 3). As indicated in Table 4, the PSO-LSTM achieved an MAE of 59.885 Wh and an RMSE of 83.783 Wh, notably better than LSTM 1 (MAE: 101.014 Wh, RMSE: 142.946 Wh), LSTM 2 (MAE: 99.441 Wh, RMSE: 139.156 Wh), and LSTM 3 (MAE: 101.971 Wh, RMSE: 141.756 Wh). The PSO algorithm's systematic optimization of key hyperparameters such as the number of hidden neurons, dropout rate, and learning rate enabled the LSTM network to generalize more effectively and reduce overfitting, thereby enhancing forecasting robustness.

Figure 4 illustrates the PSO-LSTM's performance over 24 hours. The model's forecastings (Fig. 4a) exhibit near-perfect alignment with actual consumption, even during abrupt load changes. The APE distribution (Fig. 4b) further highlights the model's consistency, with errors remaining below 8% across all hours. In contrast, existing LSTM models displayed higher and more erratic errors, particularly during morning and evening demand spikes. This improvement can be attributed to the PSO-driven hyperparameter configuration, which optimally balances model complexity and computational efficiency.

Table 3. The hyperparameters of Exciting LSTM models.

Algorithm	Parameters	Values
LSTM 1[20]	Number of hidden neurons Epochs Batch size	20 150 -
LSTM 2[21]	Number of hidden neurons Epochs Batch size	100 150 125
LSTM 3[22]	Number of hidden neurons Epochs Batch size	30 50 50

Table 4. Comparison of the PSO-LSTM model with Exciting LSTM models.

Algorithm	MAE [Wh]	RMSE [Wh]
LSTM 1	101.014	142.946
LSTM 2	99.441	139.156
LSTM 3	101.971	141.756
PSO-LSTM	59.885	83.783

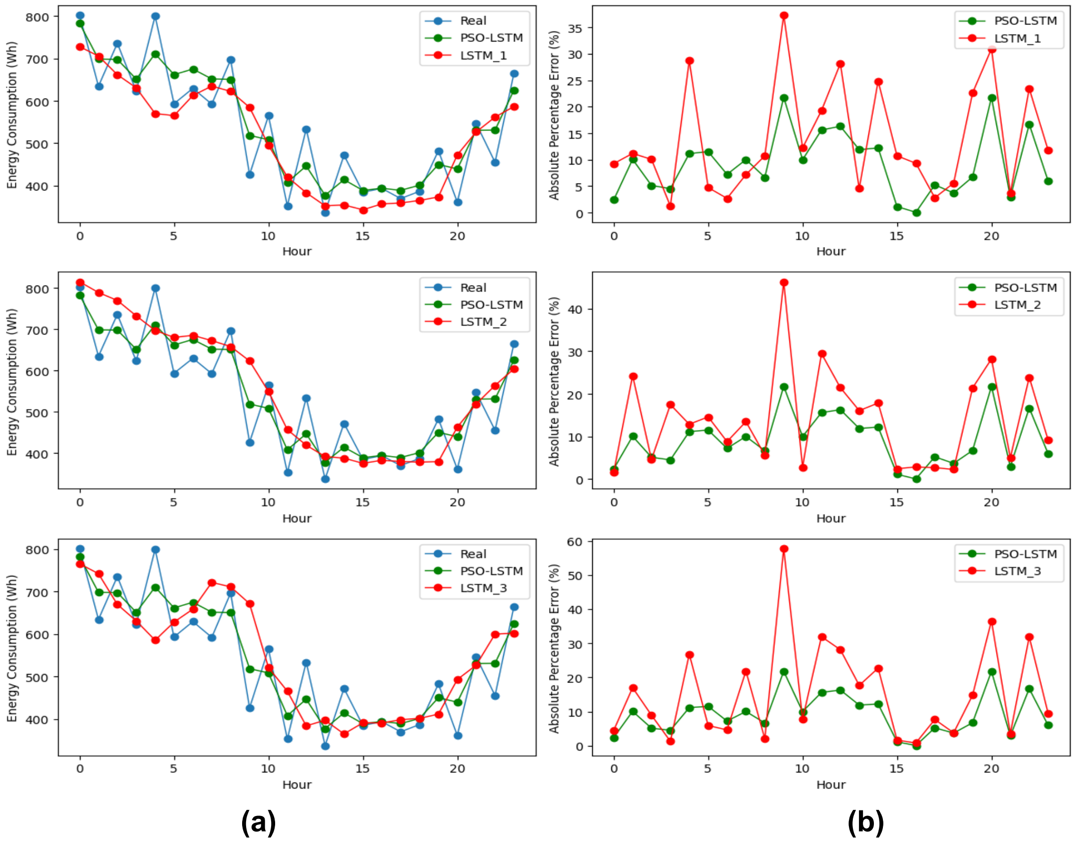

Fig. 2. The performance of the PSO-LSTM model and the exciting LSTM models. (a) Real energy consumption and energy forecastings over a full day. (b) Absolute Percentage Error in energy forecasting throughout the day.

4. CONCLUSIONS

This study demonstrates the effectiveness of a hybrid PSO-LSTM model for predicting energy use in renewable-powered microgrids. By combining PSO with LSTM networks, the approach achieved a 41.6% reduction in MAE and a 41.7% decrease in RMSE compared to standard LSTM models. These findings emphasize the importance of systematic hyperparameter tuning in improving forecasting accuracy, especially for microgrids with variable renewable outputs and fluctuating loads. The model performed reliably during peak demand periods, keeping absolute percentage errors below 8%, whereas baseline methods ranged from 12-15%, confirming its suitability for real-world conditions. The research makes a significant contribution to smart grid management by introducing a scalable framework for optimizing deep learning models in energy forecasting. The elimination of manual trial-and-error tuning through PSO improves efficiency and ensures reproducibility across diverse microgrid configurations. Empirical validation using data from the Roche Plate microgrid demonstrates the model's practical applicability in regions with limited grid connectivity, where accurate forecasting is essential for reducing reliance on fossil fuels and stabilizing energy supply. The quantified operational benefits, including a potential 9.5% reduction in energy costs for microgrid operators, further emphasize the economic value of this approach.

While the study shows promising results, certain limitations warrant attention. The model's performance may depend on retuning when applied to microgrids with significantly different infrastructure or load profiles, and its accuracy could potentially benefit from integrating additional contextual data, such as occupancy patterns or socioeconomic factors. Future research should explore transfer learning techniques to enhance cross-microgrid adaptability and extend the forecasting horizon to 24-48 hours for improved long-term planning. Integrating the model with real-time control systems could also unlock new opportunities for automated demand response and grid resilience. By addressing the unique challenges of isolated energy systems, this work advances global efforts toward sustainable energy transition. The PSO-LSTM framework provides a foundational tool for communities striving for energy self-sufficiency, particularly in regions vulnerable to climate change and energy poverty. As renewable penetration increases worldwide, the presented methodology offers a scalable pathway to optimize grid operations and reduce carbon footprints.

REFERENCES

[1] M. Akpan, A. Adebayo, “Artificial intelligence and the dual paradoxes: examining the interpla y of efficiency, resource consumption, and labor dynamics,” *arXiv*, 2025, doi: 10.48550/arXiv.2504.10503.

[2] D. Ochoa-Correa, P. Arévalo, S. Martinez, “Pathways to 100% renewable energy in island systems: a systematic review of challenges, solutions strategies, and success cases,” *Technologies*, vol. 13, no. 5, p. 180, 2025, doi: 10.3390/technologies13050180.

[3] S. Selosse, O. Ricci, S. Garabedian, N. Maïzi, “Exploring sustainable energy future in Reunion island,” *Util Policy*, vol. 55, pp. 158–166, 2018, doi: 10.1016/j.jup.2018.10.006.

[4] W. Figueredo, O. Saavedra, P. Neto, D.Oliveira, “Design and operational challenges of renewable-powered isolated microgrids: a zero-carbon approach,” *Scientific Reports,* vol. 15, no. 1, p. 45296, 2025, doi: 10.1038/s41598-025-28882-x.

[5] A. Taha, P. Makeen, N. Nazih, “Short-term and long-term solar irradiance forecasting with advanced machine learning techniques in Zafarana, Egypt,” *Scientific Reports*, vol. 15, no. 1, p. 39553, 2025, doi: 10.1038/s41598-025-24853-4.

[6] J. Wojtkiewicz, M. Hosseini, R. Gottumukkala, T. Chambers, “Hour-ahead solar irradiance forecasting using multivariate gated recurrent units,” *Energies*, vol. 12, no. 21, p. 4055, 2019, doi: 10.3390/en12214055.

[7] M. Abdelsattar, M. Azim, A. AbdelMoety, A. Emad-Eldeen, "Comparative analysis of deep learning architectures in solar power prediction," *Scientific Reports*, vol. 15, no. 1, p. 31729, 2025, doi: 10.1038/s41598-025-14908-x.

[8] M. Sabri, M. El-Hassouni, "A novel deep learning approach for short term photovoltaic power forecasting based on GRU-CNN model," E3S Web of Conferences, 2022, doi: 10.1051/e3sconf/202233600064.

[9] Y. Wang, W. Liao, Y. Chang, "Gated recurrent unit network-based short-term photovoltaic forecasting," *Energies*, vol. 11, no. 8, p. 2163, 2018, doi: 10.3390/en11082163.

[10] J. Cheng, D. Duan, X. Cheng, L. Yang, S. Cui, "Adaptive control for energy exchange with probabilistic interval predictors in isolated microgrids," *Energies*, vol. 14, no. 2, 2021, doi: 10.3390/en14020375.

[11] M. Ibrahim, S. Gharghory, H. Kamal, "A hybrid model of CNN and LSTM autoencoder-based short-term PV power generation forecasting," *Electrical Engineering*, vol. 106, no. 4, pp. 4239–4255, 2024, doi: 10.1007/s00202-023-02220-8.

[12] L. Oumiguil, A. Nejmi, "A daily PV plant power forecasting using eXtreme gradient boosting algorithm," 5th International Conference on Innovative Research in Applied Science, Engineering and Technology, 2025, doi: 10.1109/IRASET64571.2025.11008237.

[13] N. Dimitropoulos *et al.*, "Forecasting of short-term PV production in energy communities through machine learning and deep learning algorithms," 12th International Conference on Information, Intelligence, Systems & Applications, 2021, doi: 10.1109/IISA52424.2021.9555544.

[14] E. Al-Ali *et al.*, "Solar energy production forecasting based on a hybrid CNN-LSTM-transformer model," *Mathematics*, vol. 11, no. 3, p. 676, 2023, doi: 10.3390/math11030676.

[15] L. Oumiguil, A. Nejmi, "Forecasting energy consumption on a microgrid using ARIMA-GRU model," *Solar Energy and Sustainable Development Journal*, vol. 14, pp. 15–26, 2025, doi: 10.51646/jsesd.v14iSTR2E.791.

[16] D. Calogine, J. Francou, C. Abbezzot, T. Fanjirindratovo, "Data in experimental stand-alone microgrid: Solar production, domestic loads, battery storage and meteorological series," *Data Brief*, vol. 51, p. 109643, 2023, doi: 10.1016/j.dib.2023.109643.

[17] M. Tovar, M. Robles, F. Rashid, "PV power prediction, using CNN-LSTM hybrid neural network model. case of study: Temixco-Morelos, México," *Energies*, vol. 13, no. 24, 2020, doi: 10.3390/en13246512.

[18] E. Souza, D. Santos, G. Oliveira, A. Silva, A. Oliveira, "Swarm optimization clustering methods for opinion mining," *Nature Computational Science*, vol. 19, no. 3, pp. 547–575, 2020, doi: 10.1007/s11047-018-9681-2.

[19] H. Khoshvaght, R. Permala, A. Razmjou, M. Khiadani, "A critical review on selecting performance evaluation metrics for supervised machine learning models in wastewater quality prediction," *Journal of Environmental Chemical Engineering*, vol. 13, no. 6, p. 119675, 2025, doi: 10.1016/j.jece.2025.119675.

[20] S. Bouktif, A. Fiaz, A. Ouni, M. A. Serhani, "Optimal deep learning LSTM model for electric load forecasting using feature selection and genetic algorithm: comparison with machine learning approaches," *Energies*, vol. 11, no. 7, 2018, doi: 10.3390/en11071636.

[21] X. Qing, Y. Niu, "Hourly day-ahead solar irradiance prediction using weather forecasts by LSTM," *Energy*, vol. 148, pp. 461–468, 2018, doi: 10.1016/j.energy.2018.01.177.

[22] W. Kong, Z. Dong, Y. Jia, D. Hill, Y. Xu, Y. Zhang, "Short-term residential load forecasting based on LSTM recurrent neural network," *IEEE Transactions on Smart Grid*, vol. 10, no. 1, pp. 841–851, 2019, doi: 10.1109/TSG.2017.2753802.